




# All-Optical Regeneration and Format Conversion for 4APSK Signals Based on Nonlinear Effects in HNLF

Qiankun Li , Huashun Wen , Jiali Yang, Qi Xu, Xiongwei Yang , and Yameng Li

**Abstract**—An all-optical format conversion and regeneration scheme about 4-ary amplitude and phase shift keying (4APSK) signals is proposed and numerically simulated based on nonlinear effects in the high nonlinear fiber (HNLF). The input 4APSK signal is firstly converted into a regular quadrature phase shift keying (QPSK) signal by the nonlinear Mach-Zehnder interferometer (MZI) based on the self-phase modulation (SPM). Secondly, a degenerate phase-sensitive amplification (PSA) based on the four-wave mixing (FWM) is utilized to convert the regular-QPSK into two binary phase shift keying (BPSK) signals. The nonlinear MZI configuration is also used to compress the amplitude noise of BPSK. Thirdly, one phase shifter and one variable optical attenuator (VOA) are used to adjust the relative phase and power relationships of the two amplitude-regenerated BPSK signals. The regenerated 4APSK and converted QPSK signals can be generated in one 3-dB optical coupler through coherent addition of the two regenerated BPSK signals. The error-vector-magnitude (EVM) and the bit-error-rate (BER) are calculated and compared to evaluate the scheme performance. The proposed scheme can be applied as an optical regenerator or format converter at the network gateway to increase the transmission distance or connect optical networks with different modulation formats.

**Index Terms**—Quadrature phase shift keying, amplitude and phase shift keying, self-phase modulation, four-wave mixing, nonlinear Mach-Zehnder interferometer, phase-sensitive amplification.

## I. INTRODUCTION

WITH the development of emerging technologies and services, including the Internet of Energy (IoE), the Internet of Things (IoT), the Big Data, the cloud computing,

Manuscript received 16 December 2022; revised 3 January 2023; accepted 8 January 2023. Date of publication 10 January 2023; date of current version 18 January 2023. This work was supported by the National Key R&D Program of China under Grants 2019YFB2203104 and 2020YFB2205801. (Corresponding authors: Qiankun Li; Huashun Wen.)

Qiankun Li is with the School of Physics, University of Electronic Science and Technology of China, Chengdu 610054, China (e-mail: liqk@bupt.cn).

Huashun Wen is with the State Key Laboratory on Integrated Optoelectronics, Institute of Semiconductors, Chinese Academy Sciences, Beijing 10083, China, and also with the School of Electronic, Electrical and Communication Engineering, University of Chinese Academy of Sciences, Beijing 100049, China (e-mail: whs@semi.ac.cn).

Jiali Yang is with the School of Information and Communication Engineering, Beijing University of Posts and Telecommunications, Beijing 100876, China (e-mail: yangjiali@bupt.edu.cn).

Qi Xu is with the School of Information and Electronics, Beijing Institute of Technology, Beijing 100081, China (e-mail: 3220215105@bit.edu.cn).

Xiongwei Yang is with the School of Information and Technology, Fudan University, Shanghai 200433, China (e-mail: 1901200068@stu.xupt.edu.cn).

Yameng Li is with the School of Environment, Tsinghua University, Beijing 10084, China (e-mail: lymxin@126.com).

Digital Object Identifier 10.1109/JPHOT.2023.3235905

the artificial intelligence (AI) and the fifth-generation (5 G) mobile communication technology, the data traffic is growing explosively in the optical communication networks [1], [2]. For example, in the era of IoT, a large number of intelligent terminals adopt wireless and wired communication methods to connect the data flow generated to the optical transport network (OTN). Therefore, the high-speed optical signal processing function is crucial to the timely transmission of data between intelligent terminals on IoT. The underlying optical network as data transmission carries the transmission and exchange of the massive data. Therefore, improving the signal processing function of optical nodes and reducing the signal processing delay of that become the critical issues to improve the performance of IoT. The different modulation formats are allocated to the different types of optical networks to relieve the traffic pressure. The advanced modulation formats with higher spectral efficiency (SE) and chromatic dispersion (CD) tolerance can be used in the backbone optical network (BON) to improve the transmission capacity. Besides, coherent detection can enhance the receiver sensitivity and various digital signal processing (DSP) algorithms can also be used to compensate for the linear and nonlinear transmission penalties. The simple modulation formats can be used in the local access network (LAN) and the metro access network (MAN). Additionally, the direct detection method is helpful to reduce the cost per bit especially for the amounts of users and terminals [3], [4], [5]. When the optical signal is transmitted between the optical networks, the network node as a links relay node may have the ability to regenerate the optical signals, so as to increase the transmission distance. The intermediate node between different optical networks may have the format conversion function for the optical signals, so as to adopt the appropriate modulation formats flexibly according to the network size, cost, capacity and receiver devices etc.

The traditional optical signal processing in the optical network nodes includes the optical-to-electrical (OE) conversion and the electrical-to-optical (EO) conversion. However, the bottleneck of electric rate will limit the improvement of the transmission rate in the optical network nodes [6]. All-optical signal processing (AOSP) technology based on nonlinear effects has been one of the key functions in the next elastic optical network (EON) [6]. The common nonlinear effects include self-phase modulation (SPM), cross-phase modulation (XPM) and four-wave mixing (FWM) arising from the third-order nonlinear susceptibility  $\chi^{(3)}$  in the nonlinear media. All-optical regeneration and format conversion processing based on nonlinear effects can avoid the OE and EO conversions. Besides, these nonlinear effects have a

response time at the femtosecond level. Then high-speed optical transmission and switching in the optical network nodes can be realized through constructing the all-optical network nodes.

The traditional optical network nodes processing usually focuses on only one function: regeneration, format conversion, switching or others. The novel all-optical network nodes should equip with the two functions at least such as signal forwarding, format conversion, regeneration and so on. It is crucial that the optical network nodes need to be capable of format conversion and signal regeneration simultaneously in the next generation of flexible optical networks (FONs) [7]. On one hand, it allows the network intermediate nodes to select the appropriate modulation formats according to the actual needs of different types of optical networks, for instance, size, cost and traffic. On the other hand, it can extend the transmission distance of the optical signals without a power relay, after the optical signals are regenerated in the optical domain at the network links nodes.

The 4-ary amplitude and phase shift keying (4APSK) signal, as one of the quaternary modulation formats, has the higher SE and the bigger transmission capacity than the on-off keying (OOK) signal and the binary phase shift keying (BPSK) signal. It can be received by the direct detection and the coherent detection, which is suitable for the long-haul and the short-term optical transmission networks [8], [9], [10], [11]. The polarization division multiplexing QPSK (PDM-QPSK) signal is another quaternary modulation format which has been recognized as the standard modulation format for 100 G wide area network (WAN) transponders in the long-haul optical communication networks [12], [13]. Additionally, the performance analysis of the 4APSK and the differential quadrature phase shift keying (DQPSK) signals have been investigated in the linear and non-linear transmission [14].

Whether in the network intermediate nodes or in the network links nodes, there have been many articles talking about the format conversion from the 4APSK to the QPSK signals and the regeneration of 4APSK signals based on nonlinear effects and coherent addition. H. Kishikawa et al. have used the SPM effect and the saturation effect of the semiconductor optical amplifier (SOA) to realize the format conversion from the 4APSK signal to the QPSK signal [15]. L. Qiankun et al. have reported the all de-aggregation scheme from one 4APSK signal to two BPSK signals based on SPM and XPM effects [16]. However, the SOA used in the former scheme is an active device and the amplitude states of the converted QPSK can't be adjusted to be equal flexibly due to the saturation effect of SOA. The converted two BPSK signals in the latter scheme are not at the same frequency, so that an extra frequency shifting configuration is needed to ensure the coherent addition of the two converted BPSK signals.

There are also some schemes talking about the regeneration of the 4APSK signal. Mable P. Fok et al. have improved an amplitude regeneration method based on the XPM effect in a SOA [17]. T. Richter et al. have reported a phase regeneration scheme of the 4APSK signal based on the phase-sensitive amplification (PSA) [18]. Fan S. et al. have improved a phase preservation and amplitude regeneration scheme through the nonlinear optical loop mirror (NOLM) [19]. However, the existing three regeneration schemes can't realize the amplitude and

phase regeneration simultaneously. Besides, the optical signal wavelength before and after regeneration in the former scheme is deflected, which means that an extra wavelength conversion configuration is needed. These above schemes can only realize one function of the signal regeneration or the format conversion each time. In the future optical networks, the reconfigurable and multi-functional network nodes with the signal regeneration and the format conversion are more and more needed. G. Mingyi et al. have reported an format conversion from one QPSK signal to one 4APSK signal based on the PSA technology according to the orientation of the PSA gain axis [20]. C. Jiabin et al. have improved a reconfigurable and multi-functional network node to realize the format conversion from a QPSK signal to a 4APSK signal and the regeneration of the QPSK signal simultaneously [7]. However, to the best of our knowledge, the inverse function scheme about the format conversion from a 4APSK to a QPSK signal and the regeneration of the 4APSK signal simultaneously hasn't been reported.

In this paper, the reconfigurable and multi-functional optical network nodes with the signal regeneration and the format conversion capabilities about the 4APSK signal is proposed. The input 4APSK signal can be converted to a QPSK signal and regenerated based on nonlinear effects and coherent addition. In the format conversion process, the input 4APSK signal is firstly injected into one HNLF to get the distorted QPSK signal through the SPM effect. The distorted QPSK signal is sent into a nonlinear Mach-Zehnder interference (MZI) configuration to get the regular QPSK signal, which has an equal amplitude for the constellations with different phases. The PSA technology based on the FWM effect is adopted to decompose the regular QPSK signal into two BPSK signals, which are called the in-phase and quadrature components of the regular QPSK signal. The phase noise of the regular QPSK signal is compressed and converted to the amplitude noise of the BPSK signal. Thirdly, another nonlinear MZI configuration is used to regenerate the amplitude noise of the decomposed BPSK signals. At last, The VOA and the phase shifter are used to change the power and the phase states of the two regenerated BPSK signals. The regenerated 4APSK signal and the converted QPSK signal can be extracted through coherent addition of the two regenerated BPSK signals in one 3-dB optical coupler (OC). Then the format conversion from a 4APSK to a QPSK and the regeneration of the 4APSK signal are realized based on nonlinear effects including FWM and SPM. The proposed scheme is verified by theoretical and numerical simulations. The error-vector-magnitude (EVM) and bit-error-rate (BER) performance are measured to evaluate the scheme performance.

## II. THEORY AND OPERATING PRINCIPLE

In the following sections, the format conversion and the regeneration principles of the 4APSK signal are explained in detail. Section A includes one piece of HNLF and one nonlinear MZI configuration, which are used to convert the input 4APSK signal into the regular QPSK signal based on the SPM effect. Section B includes the PSA and nonlinear MZI configurations. The former is deployed to decompose the regular QPSK signal

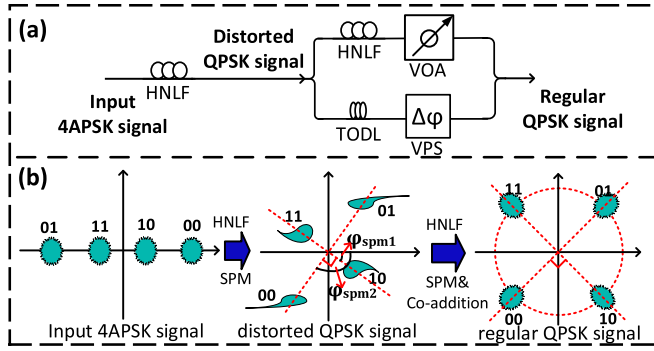


Fig. 1. The conversion scheme and the constellations from the input 4APSK signal to the regular QPSK signal, Co-addition: coherent addition.

into two in-phase and quadrature components, which can be viewed as the phase regeneration for the regular QPSK signal. The latter is used to eliminate the amplitude noise of the in-phase and quadrature components of the regular QPSK signal, that is, the amplitude regeneration for the two decomposed BPSK signals. Section C is formed by the VOA, the phase shifter and the OC. The regenerated 4APSK signal and the converted QPSK signal can be extracted from OC by adjusting the power and the relative phase states of the two regenerated in-phase and quadrature components.

#### A. The Principle of Converting the 4APSK Signal Into the Regular QPSK Signal

The format conversion scheme from the 4APSK signal to the regular QPSK signal is plotted in Fig. 1(a). Firstly, the input 4APSK signal is amplified and injected into a HNLFF. The induced SPM phase shift is added to the input 4APSK signal, then the distorted QPSK (dis-QPSK) signal is obtained, which has four phase states and two amplitude states, as shown in Fig. 1(b). The outer ring constellations of the 4APSK signal have the high intensities leading to a high SPM phase shift. While the inner ring constellations of the 4APSK signal have the low intensities leading to a low SPM phase shift. After adjusting the length of HNLFF and the power of the input 4APSK signal, the outer ring constellations of the input 4APSK will generate an extra phase shift of  $\pi/2$  compared to the inner ring constellations. The connection between the constellation points coded (10) and (11) is vertical to the connection between the constellation points coded (00) and (01), as shown in Fig. 1(b).

The adjacent constellations of the input 4APSK signal is equal interval, the ratio of the inner and the outer ring amplitudes is 1:3. The power ratio of the inner and the outer ring constellations is 1:9. The SPM phase shift added to the input 4APSK signal can be written as:

$$\varphi_{spm} = \gamma L_{eff} P \quad (1)$$

The SPM phase shift induced by the inner and the outer ring constellations of the input 4APSK signal can be expressed as:

$$\varphi_{inner} = \gamma L_{eff} P_{inner} \quad (2)$$

$$\varphi_{outer} = \gamma L_{eff} P_{outer} \quad (3)$$

Obviously, under the condition of the same effective fiber length and the nonlinear index,  $\varphi_{outer}$  is nine times of  $\varphi_{inner}$ . In order to maintain the vertical relationship of the connection between the inner and the outer ring constellations,  $\varphi_{outer}$  and  $\varphi_{inner}$  need to satisfy a particular phase relationship:

$$\varphi_{outer} - \varphi_{inner} = \pi/2 + n\pi \quad (4)$$

$n$  can be positive integer. Considering the whole power of the 4APSK signal can be expressed as:

$$P_s = (P_{outer} + P_{inner})/2 \quad (5)$$

The relationship between the input power and the parameters of HNLFF can be obtained through further simplifying the (4) and the (5):

$$P_s = \frac{5(2n+1)\pi}{16\gamma L_{eff}} \quad (6)$$

Specifically, when  $n$  is set to be 0, the (6) can be rewritten as:

$$P_s = \frac{5\pi}{16\gamma L_{eff}} \quad (7)$$

When the input power and the parameters of the used HNLFF satisfy this relationship, a distorted QPSK signal accompanying two amplitude states and four phase states with a vertical relationship of the connection between the inner and the outer ring constellations can be obtained.

Secondly, the distorted QPSK signal is sent into a nonlinear MZI configuration which is used to adjust the distribution of amplitude and phase states of the distorted QPSK signal. A nonlinear MZI configuration has been used to finish the amplitude regeneration for the pulse amplitude modulation (PAM) signal and the amplitude difference erasure for the 8-ary quadrature amplitude modulation (8QAM) signal [4], [21], [22]. It's formed by one HNLFF and one VOA in the upper arm, one variable phase shifter (VPS) and one tunable optical delay line (TODL) in the lower arm. The distorted QPSK signal can obtain a new nonlinear phase shift when it is transmitted in the nonlinear MZI configuration. Since the nonlinear index of the HNLFF used is much more higher than the TODL, the nonlinear phase shift brought by the TODL in the lower arm could be ignored compared to that induced by HNLFF in the upper arm. The outer ring amplitude constellations may obtain a higher SPM phase shift, whereas the inner ring amplitude constellations will generate a lower SPM phase shift. When the input optical signals itself with and without the SPM phase shift are coherently superposed, the outer ring amplitude constellations may obtain a bigger negative gain to reduce the amplitude, whereas the inner ring amplitude constellations may obtain a smaller negative gain to decrease the amplitude [4], [7]. In this way, the inner and outer ring amplitudes of the distorted QPSK signal can be adjusted to be equal, which is called the regular QPSK (regu-QPSK) signal. In the upper arm of the nonlinear MZI configuration, one VOA is used to change the power of the distorted QPSK signal with the SPM phase shift. A VPS in the lower arm is used to compensate for the time delay induced by the upper arm and adjust the phase of the distorted QPSK signal without the SPM phase shift, which aims to make the distorted QPSK signal with and without the



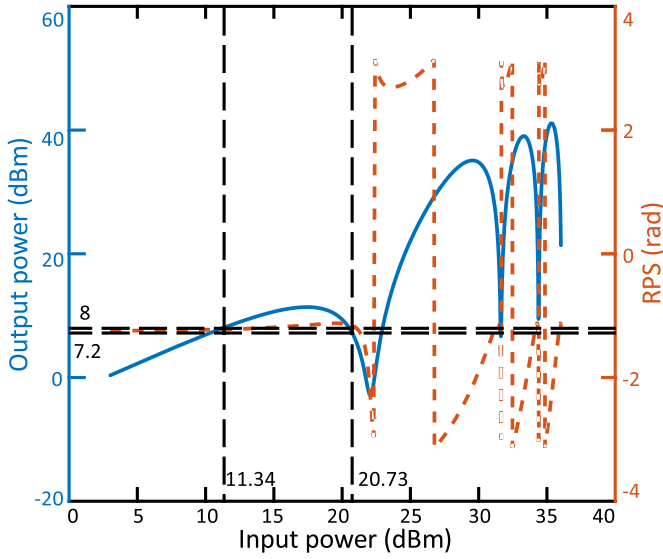


Fig. 2. The PTF and the RPS of the nonlinear MZI configuration.

SPM phase shift at the upper and lower arm coherently adding effectively. Then the format conversion from the 4APSK to the QPSK signals is finished. The regular QPSK signal has four phase states of  $\pi/4$ ,  $3\pi/4$ ,  $-3\pi/4$  and  $-\pi/4$  and one amplitude state, as shown in Fig. 1(b).

In order to interpret this format conversion from the distorted QPSK signal to the regular QPSK signal, the power transfer function (PTF) and relative phase shift (RPS) between the input and output optical signals are derived as follows [22]:

$$P_{out} = \frac{1}{4}P_{in}[1 + 10^{-\frac{\alpha}{10}} - 2 \cdot 10^{-\frac{\alpha}{20}} \cdot \cos(\varphi_{spm} + \Delta\varphi_L)] \quad (8)$$

$$\Delta\varphi_t = \arctan \frac{10^{-\frac{\alpha}{20}} \cdot \sin\varphi_{spm} + \sin\Delta\varphi_L}{10^{-\frac{\alpha}{20}} \cdot \cos\varphi_{spm} - \cos\Delta\varphi_L} \quad (9)$$

Where  $P_{in}$  and  $P_{out}$  are the input and the output optical power.  $\alpha$  and  $\Delta\varphi_L$  represent the VOA in the upper arm and the VPS in the lower arm. The PTF and the RPS curves are plotted in Fig. 2. For the distorted QPSK signal with the power of 18.2 dBm, the corresponding inner and outer level are about 11.34 dBm and 20.73 dBm, respectively. The corresponding output power are 8 dBm and 7.2 dBm for the input outer and the input inner power level. Obviously, there is only about 0.8 dB gap between the inner and the outer power level. The amplitude and the phase noise of the outer ring constellations of the distorted QPSK signal are higher than the inner ring constellations due to the SPM phase shift, as shown in Fig. 3. The 0.8 dB power gap can be ignored, namely, the output power of the corresponding inner and outer power level can be viewed as the same. Additionally, the corresponding RPS of the input inner and the outer power level are almost the same, which means the output phases of the corresponding inner and the outer constellations don't change. The converted regular QPSK signal remains the same phase states as the distorted QPSK signal.

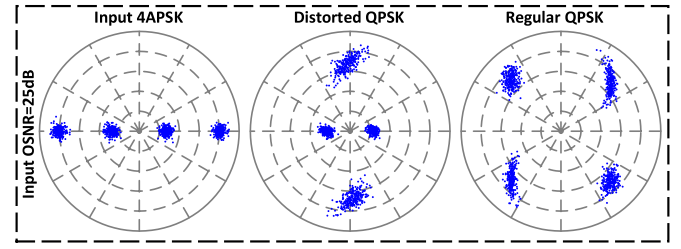


Fig. 3. Constellations of the input 4APSK, the distorted QPSK and the regular QPSK signals.

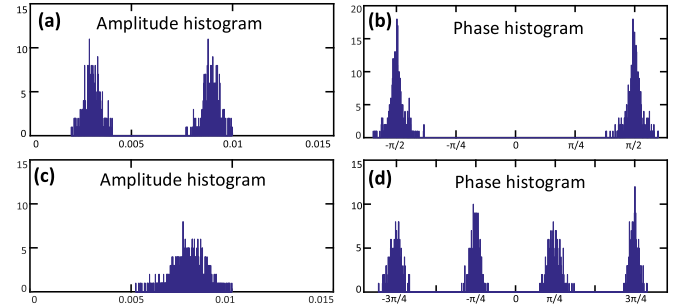


Fig. 4. Amplitude and phase histograms of the input 4APSK and the converted regular QPSK signals.

According to the above analysis, taking the input 4APSK signal with an OSNR of 25 dB as an example, the constellations of the input 4APSK, the distorted QPSK and the regular QPSK signals are plotted in Fig. 3. It can be clearly seen that the input 4APSK signal is converted into a regular QPSK signal successfully. When the input 4APSK signal is transmitted into one HNLFF, the distorted QPSK signal has more phase and amplitude noise due to the SPM effect induced by the inner and the outer ring constellations. The following nonlinear MZI configuration is used to eliminate the amplitude difference between the inner and the outer ring constellations by utilizing the induced SPM phase shift and coherent addition. Besides, the amplitude and phase histograms of the input 4APSK and the regular QPSK signals are drawn in Fig. 4. The two amplitude states of the input 4APSK signal are compressed into one amplitude of the regular QPSK signal, as shown in Fig. 4(a) and (c). While the two phase states of the input 4APSK signal are converted into four phase states of the regular QPSK signal, as shown in Fig. 4(b) and (d). These results indicate that the converted regular QPSK signal has one union amplitude and four average phase states, which is consistent with the ideal QPSK signal.

### B. The Principle of Converting the Regular QPSK Signal Into Two Regenerated BPSK Signals

From the signal constellations in Fig. 3 and the amplitude and phase histograms in Fig. 4, the quality of the regular QPSK signal is worse than that of the input 4APSK signal. In order to improve the quality of the regular QPSK signal, the amplitude regeneration and the phase regeneration are needed. The PSA technology has been investigated to realize the all-optical

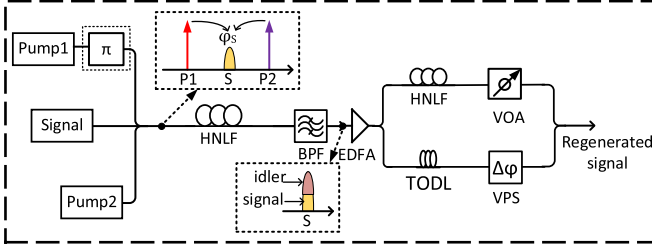


Fig. 5. The PSA and the nonlinear MZI configurations.

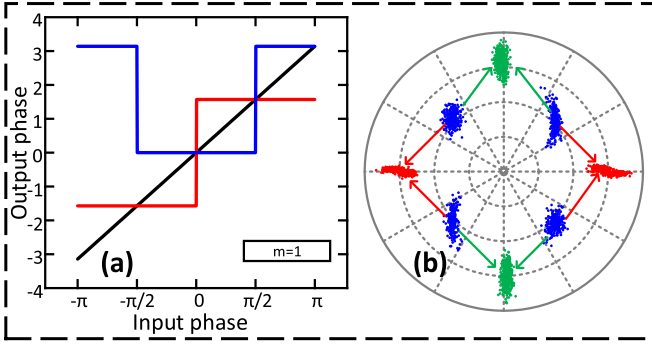


Fig. 6. Phase transfer function of the PSA. (b) Constellations of the regular QPSK signal before and after the PSA.

quantification for the all-phase signal [23], [24]. This technique has also been utilized to eliminate the phase noise of the input noisy optical signal through nonlinear wave-mixing [25], [26]. The typical quantification formula can be expressed as:

$$A_{out}e^{j\varphi_{out}} = A_{in}e^{j\varphi_{in}} + m \cdot A_M e^{j\varphi_M} \quad (10)$$

Which represents the input signal itself is coherently added with its  $M$ -order harmonics.  $m$  is the amplitude ratio of the two optical waves. When  $M = -1$ , Eq. (8) means the input signal itself is coherently added with its conjugate wave. This represents the two-level quantification for the input signal, which can be used in the format conversion and the regeneration [4], [23]. A typical degenerate PSA configuration is used in this scheme to decompose the quadrature modulation signal into the in-phase and quadrature components, as shown in Fig. 4. Two pump lights are symmetrically distributed relative to the input optical signal. Generally, assuming the phase of the optical pumps is 0, a conjugation wave will be generated at the same frequency of the input signal through the degenerate FWM effect.

When  $m$  is adjusted to 1, the input all-phase optical signal is quantized ideally to obtain the in-phase component with two phase states of 0 and  $\pi$ , as shown in Fig. 6(a). For the input QPSK signal, the four phase states of  $\pi/4$ ,  $3\pi/4$ ,  $-3\pi/4$  and  $-\pi/4$  would be squeezed into one BPSK signal with two phase states of 0 and  $\pi$ . When an extra phase shift of  $\pi$  is added to one of the two pump lights, the (8) can be rewritten as:

$$A_{out}e^{j\varphi_{out}} = A_{in}e^{j\varphi_{in}} - m \cdot A_M e^{j\varphi_M} \quad (11)$$

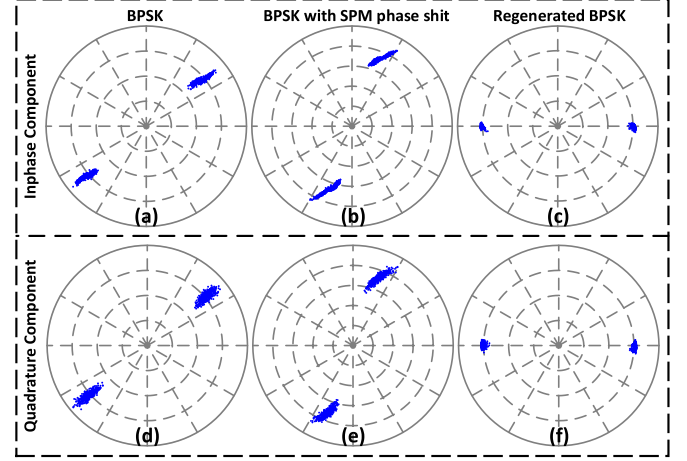


Fig. 7. Constellations of the in-phase and quadrature components before and after amplitude regeneration.

Similarly, When  $m$  is adjusted to 1, the input all-phase optical signal is quantized ideally to obtain the quadrature component with two phase states of  $\pi/2$  and  $-\pi/2$ , as shown in Fig. 6(a). For the input QPSK signal with four phase states of  $\pi/4$ ,  $3\pi/4$ ,  $-3\pi/4$  and  $-\pi/4$  would be squeezed into another BPSK signal with two phase states of  $\pi/2$  and  $-\pi/2$ . Then the QPSK signal is decomposed into two BPSK signals to eliminate its phase noise. The constellations of the regular QPSK signal and the converted in-phase and quadrature components are plotted in Fig. 6(b). This quantization progress for the regular QPSK signal can be viewed as phase regeneration processing. Moreover, the phase noise of the regular QPSK signal is converted to the amplitude noise of the two BPSK signals by the degenerate PSA.

In order to eliminate the induced amplitude noise of the decomposed BPSK signals, the other two MZI configurations are designed to compress their amplitude noise. The constellations of the two BPSK signals before and after the nonlinear MZI configurations are plotted in Fig. 7. Fig. 7(a) and (d) represent the in-phase and quadrature components of the regular QPSK signal. Fig. 7(b) and (e) represent the input in-phase and quadrature components with the SPM phase shift. Fig. 7(c) and (f) represent the regenerated in-phase and quadrature components after the nonlinear MZI configurations. We take an example of the in-phase component of the regular QPSK signal, when the BPSK signal itself with and without the SPM phase shift are coherently addition, the regenerated BPSK signal can be obtained.

### C. Obtaining the Regenerated 4APSK Signal and the Converted QPSK Signal

The QPSK and 4APSK signals as quaternary modulation signals both can be obtained through the coherent addition of the two BPSK signals. The former can be extracted when the two BPSK signals have the same power with the orthogonal relative phase states. The latter can be generated when the two BPSK signals have the same relative phase states and the amplitude ratio of 1:2. In this scheme, the VOA and the phase shifter are

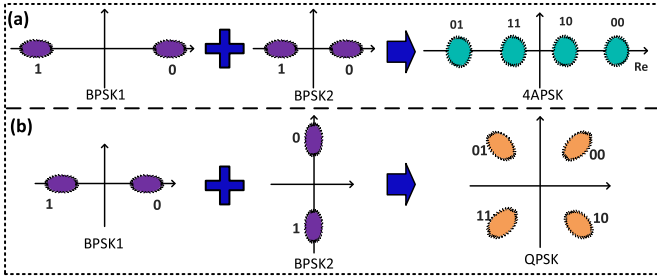


Fig. 8. Constellations of the format conversion from the BPSK to (a) the 4APSK and (b) the QPSK.

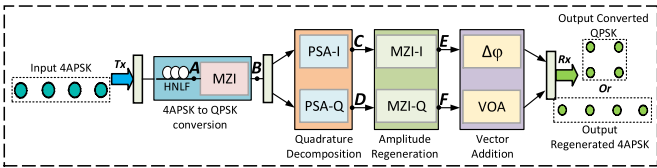


Fig. 9. Schematic diagram of the proposed scheme.

used to adjust the power and phase states of the upper and the lower arms regenerated BPSK signals. When they have the same relative phase states and 6 dB power difference, the regenerated 4APSK signal can be obtained, as shown in Fig. 8(a). When the two regenerated BPSK signals both have the same power and the orthogonal relative phase states, the converted QPSK signal can be obtained, as shown in Fig. 8(b).

### III. SIMULATIONS AND DISCUSSIONS

The proposed format conversion and regeneration scheme of the 4APSK signal is shown in Fig. 9. A seed continuous wave (CW) is injected into the phase modulators (modulated index:  $\pi$ ) and amplitude modulator (modulated index: 0.885) driven by the pseudorandom binary sequence (PRBS) to generate a 4APSK signal of 20 Gbps at the frequency of 193.1 THz. An amplified spontaneous emission (ASE) noise source is added to the 4APSK signal to change its input optical-signal-noise-ratio (OSNR). The input 4APSK signal is firstly injected into the first HNLF (HNLF1, L: 550 m) with a power of 21.3 dBm. The input 4APSK signal is converted into the distorted QPSK signal due to the phase shift brought by the SPM effect. The outer ring constellations have an extra  $\pi/2$ -phase shift compared to the inner ring constellations. Then the distorted QPSK signal (power: 18.2 dBm) is sent into a nonlinear MZI configuration to adjust the amplitude of the inner and the outer ring constellations. In the nonlinear MZI configuration, the HNLF and the VOA used in the upper arm are 370 m and 0.5 dB, respectively. The TODL and the phase shifter are set to be 340 m and  $3\pi/4$  in the lower arm to compensate for the phase shift and the time delay induced by the HNLF in the upper arm. The regular QPSK signal with the same amplitude constellations can be obtained from the nonlinear MZI configuration. The change of the constellations from the input 4APSK signal to the distorted QPSK and the regular QPSK signals are shown in Fig. 3.

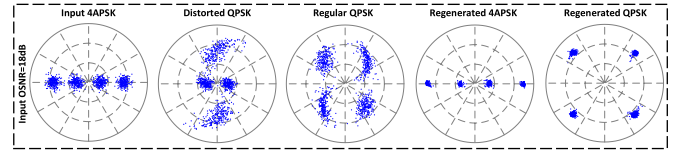


Fig. 10. Constellations of the input 4APSK signal before and after regeneration and format conversion.

There have been many reports talking about the regeneration of the QPSK signal based on the PSA [24], [25], [26], [27], [28]. In our simulation scheme, a degenerate PSA configuration with a nonlinear MZI configuration is used to convert the regular QPSK signal into two regenerated BPSK signals, which represent the in-phase and the quadrature components of the regular QPSK signal after the amplitude and the phase regeneration. The typical degenerate PSA configuration with the nonlinear MZI configuration has been depicted in Fig. 5. The used two pumps (P1 and P2) are generated by a Mach-Zehnder modulator (MZM) which is injected into a seed CW and driven by the sine wave with 30 GHz. After the regular QPSK signal (power:  $-0.9$  dBm) and two pumps (power: 18 dBm) are injected into the HNLF (L: 550 m), the in-phase component of the regular QPSK signal can be extracted. The power relationship of the regular QPSK signal and two pumps satisfies the small-signal approximation condition when the degenerate PSA is occurred. When an extra phase shift of  $\pi$  is added to one of the input two pumps, the quadrature component of the regular QPSK signal can also be extracted.

The phase noise of the regular QPSK signal is converted into the amplitude noise of the two BPSK signals after the PSA processing. The following nonlinear MZI configuration is designed to eliminate the amplitude distortion of the two BPSK signals. In this nonlinear MZI configuration, the HNLF and the VOA used in the upper arm are set to be 370 m and 1.7 dB, respectively. One TODL with the same length of 370 m is set in the lower arm of the nonlinear MZI configuration. An extra phase shift of  $3\pi/4$  is added in the lower arm of the nonlinear MZI configuration. When the in-phase and the quadrature components power are adjusted to be 18.2 dBm and 18.3 dBm, the amplitude and phase regenerated BPSK signal can be obtained. After adjusting the power and the phase relationships of the two regenerated BPSK signals, the regenerated QPSK and 4APSK signals can be obtained by coherent addition. When the phases of the two regenerated BPSK signals are orthogonal and the powers are equal, the regenerated QPSK signal can be acquired. When the phases of the two BPSK signals are the same and the amplitude ratio is 1:2, the regenerated 4APSK signal can be obtained. In the simulation, the utilized HNLF have the same parameters except the fiber length. Its attenuation is 0.2 dB/km, the dispersion is  $1.6 \times 10^{-5}$  s/m<sup>2</sup>, the dispersion slope is  $0.08 \times 10^3$  s/m<sup>3</sup>, the nonlinear index is  $2.6 \times 10^{-20}$  m<sup>2</sup>/W and the effective core area is  $80 \times 10^{-13}$  m<sup>2</sup>. The constellations of the input 4APSK signal, the distorted QPSK signal, the regular QPSK signal, the regenerated 4APSK signal and the converted QPSK signal in the proposed scheme are shown in Fig. 10.

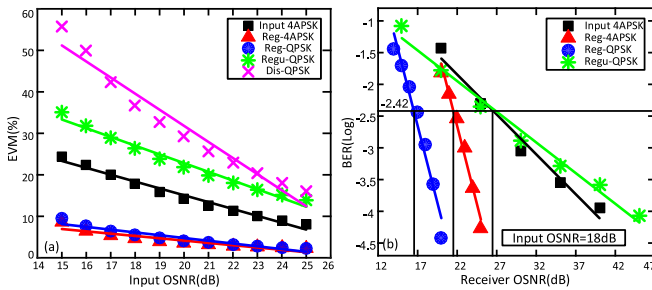


Fig. 11. (a) EVM and (b) BER performance of the scheme.

In order to evaluate the format conversion and regeneration performance of the proposed scheme, the ASE noise is added to change the receiver OSNR related to 0.1 nm noise bandwidth to simulate the actual situation of transmitting the signals in the fiber-optic links.  $2^{10}$  and  $2^{17}$  signal symbols are counted to measure the EVM and the BER performance, respectively, which are plotted in Fig. 11. With the improvement of the input OSNR in Fig. 11(a), the EVM performance of the input 4APSK signal is lower than the distorted QPSK and the regular QPSK signals. When the input 4APSK signal is transmitted into one HNLF, the distorted QPSK signal has more severe phase and amplitude noise due to the SPM effect induced by the inner and the outer ring constellations. The EVM performance of the distorted QPSK is worse than the regular QPSK signal. The designed nonlinear MZI can compress the partial amplitude noise of the distorted 4APSK signal based on the SPM and coherent addition. The regenerated 4APSK signal and the converted QPSK signal have better EVM performance than the input 4APSK signal. These results prove that the amplitude and phase noise are compressed effectively through the proposed scheme based on SPM and FWM effects.

With the input OSNR of 18 dB, at the hard decision forward error correction (HD-FEC) threshold is set to be  $\log_{10}(3.8 \times 10^{-3}) = -2.42$ , the BER transmission performance of the regenerated 4APSK signal and the converted QPSK signal are better than the input 4APSK signal, the distorted QPSK signal and the regular QPSK signal. As shown in Fig. 11(b), the regenerated 4APSK and the converted QPSK signals have about 5 dB and 10 dB improvement in receiver OSNR compared to the input 4APSK signal, respectively. This indicates the regenerated 4APSK and the converted QPSK signals have the better anti-noise ability and can extend the transmission distance longer. Moreover, the QPSK signal as a phase modulated signal has the stronger anti-noise ability than the 4APSK signal as an amplitude and phase modulated signal. This is because the 4APSK signal is more sensitive to the nonlinear phase noise induced by the SPM effect than the QPSK signal, which has the larger Euclidean distance between the adjacent constellations. It should be noteworthy that any all-optical regenerator based on the nonlinear optical processing can't be used to reduce the original BER of the input noisy optical signal. However, the original OSNR of the input noisy optical signal can be improved. The regenerated optical signal can also transmit a longer distance

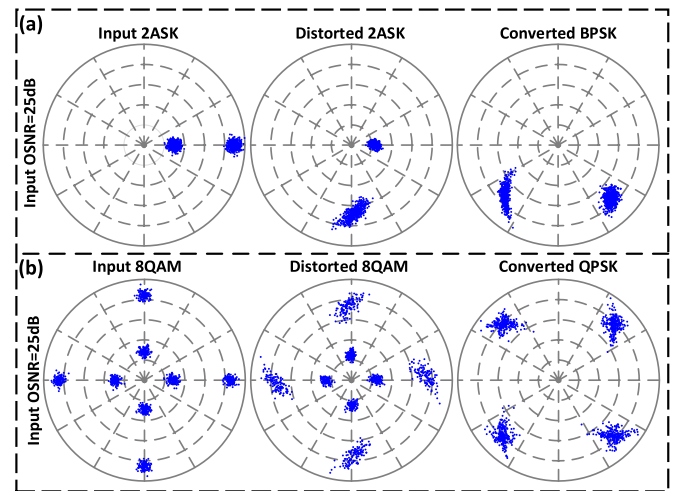


Fig. 12. Constellations of (a) the 2ASK and (b) the star-8QAM signals.

than the input noisy optical signal. Namely, under the interference of the same intensity of noise, e.g., the ASE noise, the regenerated optical signal can obtain a better BER transmission performance.

The proposed scheme has some other scalable applications in the format conversion and regeneration processing. For example, it can also be used to convert one 2ASK signal to one BPSK signal and convert one star-MQAM signal into one M/2-PSK signal by only selecting section A. For the input 2ASK signal, it is firstly converted into the distorted 2ASK signal by the first HNLF through the SPM effect. The following nonlinear MZI configuration can remove the amplitude difference between the inner and outer rings constellations of the distorted 2ASK signal. The converted BPSK signal with a phase offset of  $\pi/2$  between the different constellation diagrams can be extracted in Fig. 12(a). The format conversion advantage is that there is no wavelength conversion for the MAN and the BON, which deploy to use the ASK and the PSK signals separately [29]. For the input star-MQAM signal, it can be viewed as two 4APSK signals at the in-phase component and quadrature component directions. The distorted star-8QAM signal can be obtained after the input star-8QAM signal is sent into the first HNLF. The amplitude difference between the inner and outer rings of the distorted star-8QAM signal is erased by the nonlinear MZI configuration. The constellations of the input star-8QAM, the distorted star-8QAM and the converted QPSK signals are plotted in Fig. 12(b). The converted QPSK signal as a low-order phase modulated signal has a better anti-noise ability and the nonlinear phase noise tolerance than the star-8QAM signal.

Another application is the inverse operation that the QPSK signal can be regenerated and converted into the 4APSK signal. The input QPSK signal is sent into the first HNLF to get the distorted QPSK signal. The distorted QPSK signal is converted into the regular QPSK signal through the nonlinear MZI configuration. The regular QPSK signal is converted into two regenerated BPSK signals through the cascaded PSA and



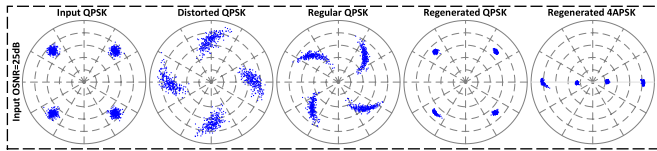


Fig. 13. Constellations of the input QPSK signal before and after regeneration and format conversion.

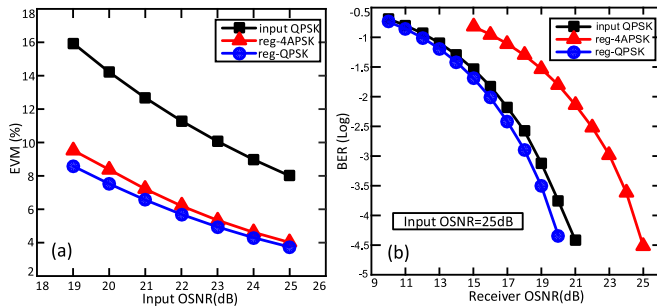


Fig. 14. (a) EVM and (b) BER performance of the scheme.

the nonlinear MZI configurations. After adjusting the power and the phase states of the two regenerated BPSK signals, the regenerated QPSK and the converted 4APSK signals can be extracted separately. The constellations of the input QPSK, the distorted QPSK, the regular QPSK, the regenerated QPSK and the converted 4APSK signals are plotted in Fig. 13. As shown in Fig. 13, the input QPSK signal is regenerated and converted to the 4APSK signal successfully. Combining the Fig. 10 and the Fig. 13, the proposed scheme can be applied in the network nodes to realize the bidirectional format conversion and regeneration for 4APSK and QPSK signals simultaneously.

The EVM and the BER performance of QPSK signals before and after regeneration and format conversion are measured in Fig. 14. With the increase of input OSNR, the EVMs of the regenerated QPSK signal and the converted 4APSK signal are lower than the input QPSK signal. This is mainly due to the amplitude and the phase noise compression based on the PSA and the nonlinear MZI configuration for the input QPSK signal. When the input OSNR is set to be 25 dB, the regenerated QPSK signal obtains a little better receiver OSNR performance improvement than the input QPSK signal at the HD-FEC threshold of  $\log_{10}(3.8 \times 10^{-3}) = -2.42$ . The regenerated 4APSK signal has a worse BER transmission performance compared to the input QPSK signal. Although the 4APSK and QPSK signals, as quaternary modulation signals, have the same spectrum efficiency, the 4APSK signal has a worse amplitude noise tolerance than the QPSK signal. When the optical signal transmits in the fiber-optic links, the ASE noise induced by optical amplifiers will bring more amplitude noise. The QPSK signal can have a better anti-noise ability than the 4APSK signal, since the Euclidean distance of the adjacent constellations for the QPSK signal is bigger than the 4APSK signal.

#### IV. CONCLUSION

In this paper, an all-optical regeneration and format conversion scheme about the input 4APSK signal based on the FWM and SPM effects in the HNLF was proposed and simulated. The regenerated 4APSK and the converted QPSK signals both have better EVM and BER performance than the input 4APSK signal. Moreover, the proposed scheme can be extended to convert a star-8QAM signal to a QPSK signal and convert an ASK signal to a PSK signal, when the Section A is selected. The system can also be used to realize the regeneration and format conversion for the input QPSK signal, which makes the scheme is applicable to the bidirectional regeneration and format conversion for the input QPSK and 4APSK signals simultaneously. Therefore, the proposed scheme can also be a regenerator and format converter for the QPSK and the 4APSK signals at the network gateway to select the appropriate modulation formats to connect optical networks or extend the fiber-optic transmission distance.

#### ACKNOWLEDGMENT

The authors acknowledge the reviewers and editors for their careful and constructive suggestions. Qiankun Li wants to thank the happiness, company, and support from his parents and friend Hao Zhang over the past years.

#### REFERENCES

- [1] Y. Ji, J. Zhang, X. Wang, and H. Yu, "Towards converged, collaborative and co-automatic (3C) optical networks," *Sci. China Inf. Sci.*, vol. 61, no. 12, 2018, Art. no. 121301.
- [2] X. Liu, "Evolution of fiber-optic transmission and networking towards the 5G era," *iScience*, vol. 22, pp. 489–506, 2019.
- [3] T. Ahmed et al., "Dynamic routing, spectrum, and modulation-format allocation in mixed-grid optical networks," *J. Opt. Commun. Netw.*, vol. 12, pp. 79–88, 2020.
- [4] Q. Li, X. Yang, and J. Yang, "All-optical aggregation and de-aggregation between 8QAM and BPSK signal based on nonlinear effects in HNLF," *J. Lightw. Technol.*, vol. 39, no. 17, pp. 5432–5438, Sep. 2021. [Online]. Available: <https://opg.optica.org/jlt/abstract.cfm?URI=jlt-39-17-5432>
- [5] Q. Li, X. Yang, H. Wen, Q. Xu, J. Yang, and H. Yang, "All-optical format conversion for Star-8QAM signals based on nonlinear effects in elastic optical networks," *J. Lightw. Technol.*, early access, Oct. 25, 2022, doi: [10.1109/JLT.2022.3216841](https://doi.org/10.1109/JLT.2022.3216841).
- [6] A. E. Willner et al., "All-optical signal processing techniques for flexible networks," *J. Lightw. Technol.*, vol. 37, no. 1, pp. 21–35, Jan. 2019. [Online]. Available: <http://opg.optica.org/jlt/abstract.cfm?URI=jlt-37-1-21>
- [7] J. Cui et al., "Reconfigurable optical network intermediate node with full-quadrature regeneration and format conversion capacity," *J. Lightw. Technol.*, vol. 36, no. 20, pp. 4691–4700, Oct. 2018. [Online]. Available: <https://opg.optica.org/jlt/abstract.cfm?URI=jlt-36-20-4691>
- [8] M. Ohm and J. Speidel, "Quaternary optical ASK-DPSK and receivers with direct detection," *IEEE Photon. Technol. Lett.*, vol. 15, no. 1, pp. 159–161, Jan. 2003.
- [9] X. Liu et al., "Return-to-zero quaternary differential-phase amplitude-shift-keying for long-haul transmission," in *Proc. Opt. Fiber Commun. Conf.*, 2004, Paper FN2. [Online]. Available: <http://www.osapublishing.org/abstract.cfm?URI=OFC-2004-FN2>
- [10] C. Häger, A. Graell i Amat, A. Alvarado, and E. Agrell, "Design of APSK constellations for coherent optical channels with nonlinear phase noise," *IEEE Trans. Commun.*, vol. 61, no. 8, pp. 3362–3373, Aug. 2013.
- [11] J. Prat, J. C. Velsquez, and J. Tabares, "Direct PSK-ASK modulation for coherent udWDM," in *Proc. IEEE 21st Int. Conf. Transparent Opt. Netw.*, 2019, pp. 1–4.
- [12] P. Winzer, "Beyond 100G ethernet," *IEEE Commun. Mag.*, vol. 48, no. 7, pp. 26–30, Jul. 2010.



- [13] H. Kishikawa, N. Goto, and L. R. Chen, "All-optical wavelength preserved modulation format conversion from PDM-QPSK to PDM-BPSK using FWM and interference," *J. Lightw. Technol.*, vol. 34, no. 23, pp. 5505–5515, Dec. 2016. [Online]. Available: <https://opg.optica.org/jlt/abstract.cfm?URI=jlt-34-23-5505>
- [14] Y. Yadin, M. Orenstein, and M. Shtaif, "Optical DPASK and DQPSK: A comparative analysis for linear and nonlinear transmission," *IEEE J. Sel. Topics Quantum Electron.*, vol. 12, no. 4, pp. 581–588, Jul./Aug. 2006.
- [15] H. Kishikawa and N. Goto, "Wavelength preserved modulation format conversion from 16QAM to QPSK using FWM and SPM," in *Proc. Conf. Lasers Electro-Opt. Pacific Rim.*, 2017, Art. no. s0962. [Online]. Available: <https://opg.optica.org/abstract.cfm?URI=CLEOPR-2017-s0962>
- [16] Q. Li and P. Zhu, "All-optical de-aggregation of 4-Level APSK to 2BPSK signals based on SPM and XPM using HNLF," in *Proc. Asia Commun. Photon. Conf.*, 2019, Art. no. M4A.57. [Online]. Available: <http://www.osapublishing.org/abstract.cfm?URI=ACPC-2019-M4A.57>
- [17] M. P. Fok, C. Shu, and D. J. Blumenthal, "All-optical ASK-DPSK signal regeneration using a semiconductor optical amplifier," in *Proc. Conf. Lasers Electro-Opt./Quantum Electron. Laser Sci. Conf. Photon. Appl. Syst. Technol.*, 2007, Art. no. JTuA126. [Online]. Available: <https://opg.optica.org/abstract.cfm?URI=CLEO-2007-JTuA126>
- [18] T. Richter, R. Elschner, and C. Schubert, "Phase-regeneration of 2ASK-BPSK in a one-mode phase-sensitive amplifier," in *Proc. IEEE Photon. Soc. Summer Topical Meeting Ser.*, 2013, pp. 157–158.
- [19] F. Sun, B. Wu, S. Zhang, and F. Wen, "All-optical rectangular-QAM regenerators based on phase-preserving I/Q shaping," *Opt. Commun.*, vol. 467, 2020, Art. no. 125634.
- [20] M. Gao, T. Kurosu, K. Solis-Trapala, T. Inoue, and S. Namiki, "Quadrature squeezing and IQ de-multiplexing of QPSK signals by sideband-assisted dual-pump phase sensitive amplifiers," *IEICE Trans. Commun.*, vol. E98.B, pp. 2227–2237, 2015.
- [21] X. Kong et al., "Design of all-optical multi-level regenerators based on Mach-Zehnder interferometer," *Opt. Commun.*, vol. 380, pp. 377–381, 2016.
- [22] Q. Li et al., "All-optical format conversion of 2-Dimensional MQAM to MPSK based on nonlinear Mach-Zehnder interferometer with wavelength preservation," *J. Lightw. Technol.*, vol. 40, no. 22, pp. 7246–7253, Nov. 2022.
- [23] R. Slavik et al., "All-optical phase and amplitude regenerator for next-generation telecommunications systems," *Nature Photon.*, vol. 4, pp. 690–695, 2010.
- [24] H. Wang, C. He, G. Li, and Y. Ji, "All-optical phase quantization with high accuracy based on a multiwave interference phase sensitive amplifier," *IEEE Photon. J.*, vol. 9, no. 3, Jun. 2017, Art. no. 7802508.
- [25] M. Gao, T. Kurosu, T. Inoue, and S. Namiki, "Low-penalty phase demultiplexing of QPSK signal by dual-pump phase sensitive amplifiers," in *Proc. IEEE 39th Eur. Conf. Exhib. Opt. Commun.*, 2013, vol. 2013, pp. 1–3.
- [26] A. Lorences-Riesgo et al., "Quadrature demultiplexing using a degenerate vector parametric amplifier," *Opt. Exp.*, vol. 22, no. 24, pp. 29424–29434, Dec. 2014. [Online]. Available: <https://opg.optica.org/oe/abstract.cfm?URI=oe-22-24-29424>
- [27] K. R. H. Bottrill, G. Hesketh, L. Jones, F. Parmigiani, D. J. Richardson, and P. Petropoulos, "Full quadrature regeneration of QPSK signals using sequential phase sensitive amplification and parametric saturation," *Opt. Exp.*, vol. 25, no. 2, pp. 696–705, Jan. 2017. [Online]. Available: <https://opg.optica.org/oe/abstract.cfm?URI=oe-25-2-696>
- [28] Z. Zheng, L. An, Z. Li, X. Zhao, and X. Liu, "All-optical regeneration of DQPSK/QPSK signals based on phase-sensitive amplification," *Opt. Commun.*, vol. 281, pp. 2755–2759, 2008.
- [29] C. Yan et al., "All-optical format conversion from NRZ to BPSK using a single saturated SOA," *IEEE Photon. Technol. Lett.*, vol. 18, no. 22, pp. 2368–2370, Nov. 2006.